Recent DMRG Study for Finite Doped t-J Ladder

Sun Rongyang

Institute for Advanced Study, Tsinghua University

April 17, 2018

Outline

1. Singlet pairing and superfluidity in t-J ladders with Mott insulating stripes [1804.00670]
2. Dynamical DMRG study of spin and charge excitations in the four-leg t-t'-J ladder [1803.11342]
3. Summary

Hamiltonian

t-J-V model

$$
\begin{aligned}
\hat{H} \quad = \quad & -t_x \sum_{\sigma} \sum_{i_x=1}^{L_x-1} \sum_{i_y=1}^{L_y} (\hat{c}^{\dagger}_{i_x,i_y,\sigma} \hat{c}_{i_x+1,i_y,\sigma} + h.c.) \\
& -t_y \sum_{\sigma} \sum_{i_x=1}^{L_x} \sum_{i_y=1}^{L_y-1} (\hat{c}^{\dagger}_{i_x,i_y,\sigma} \hat{c}_{i_x,i_y+1,\sigma} + h.c.) \\
& +J_x \sum_{i_x=1}^{L_x-1} \sum_{i_y=1}^{L_y} (\boldsymbol{S}_{i_x,i_y} \cdot \boldsymbol{S}_{i_x+1,i_y}) \\
& +J_y \sum_{i_x=1}^{L_x} \sum_{i_y=1}^{L_y-1} (\boldsymbol{S}_{i_x,i_y} \cdot \boldsymbol{S}_{i_x,i_y+1}) \\
& +\sum_{\boldsymbol{i}} V_{i_y} \hat{n}_{\boldsymbol{i}}
\end{aligned}
$$

Parameters

Model parameters

t	J_x	J_y	V	L_x	L_y	BC
1.0	0.33	0.33 0.50 0.75 1.00	-40	28	4	OBC

$$V_{i_y=2} = V_{i_y=3} = V, \; V_{i_y=1} = V_{i_y=4} = 0$$
$$N_\uparrow = N_\downarrow = \frac{1}{2} \times \frac{3}{4}(L_x L_y)$$

Simulation parameters

MaxStateNum	TruncErr
8000	10^{-7}

Geometry

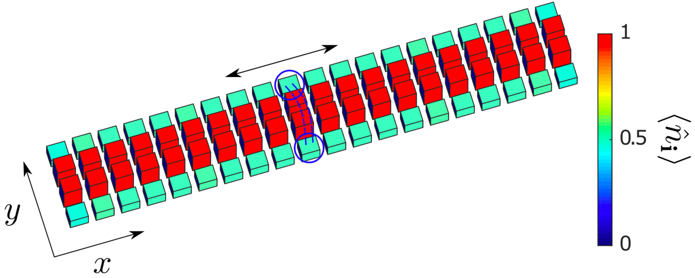

$\langle \hat{n}_i \rangle \approx 1.0$ in the inner two legs and $\langle \hat{n}_i \rangle \approx 0.5$ in the outer two legs.

Definition

$$E_b = E_0(N_\uparrow + 1, N_\downarrow + 1) + E_0(N_\uparrow, N_\downarrow) - 2E_0(N_\uparrow + 1, N_\downarrow)$$

Simulation results I

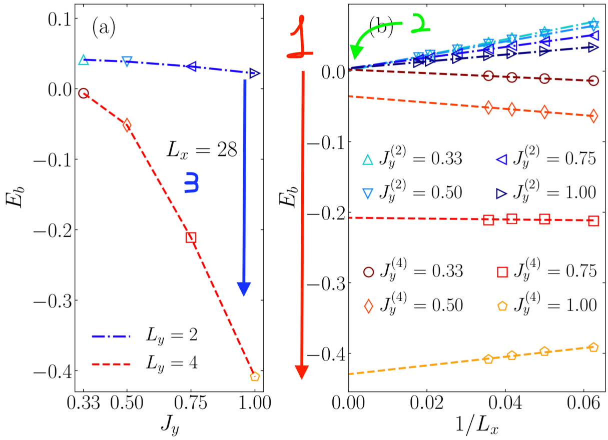

Simulation results II

1. The binding energy becomes increasingly negative as J_y increases.
2. Homogeneous two-legs ladder has positive or vanish binding energies in the thermodynamic limit.
3. The Mott stripe in between the outer two legs is necessary to observe such robust negative binding energies.

Definitions

pair correlation function

$$P_{x_1,x_2} = \langle \hat{\Delta}^\dagger_{x_1} \hat{\Delta}_{x_2} \rangle$$

Inter-leg case

$$\hat{\Delta}^\dagger_{x_1} = \begin{cases} (\hat{c}^\dagger_{x_1,1,\downarrow}\hat{c}^\dagger_{x_1,L_y,\uparrow} - \hat{c}^\dagger_{x_1,1,\uparrow}\hat{c}^\dagger_{x_1,L_y,\downarrow})/\sqrt{2} & \text{for singlet } (P^S) \\ \hat{c}^\dagger_{x_1,1,\downarrow}\hat{c}^\dagger_{x_1,L_y,\downarrow} & \text{for triplet } (P^T) \end{cases}$$

Intra-leg case

$$\hat{\Delta}^\dagger_{x_1(,y)} = \begin{cases} (\hat{c}^\dagger_{x_1,1,\downarrow}\hat{c}^\dagger_{x_1+1,1,\uparrow} - \hat{c}^\dagger_{x_1,1,\uparrow}\hat{c}^\dagger_{x_1+1,1,\downarrow})/\sqrt{2} & \text{for singlet } (P^S_{1D}) \\ \hat{c}^\dagger_{x_1,y,\downarrow}\hat{c}^\dagger_{x_1+1,y,\downarrow} & \text{for triple } (P^T_{1D}) \end{cases}$$

Simulation results I

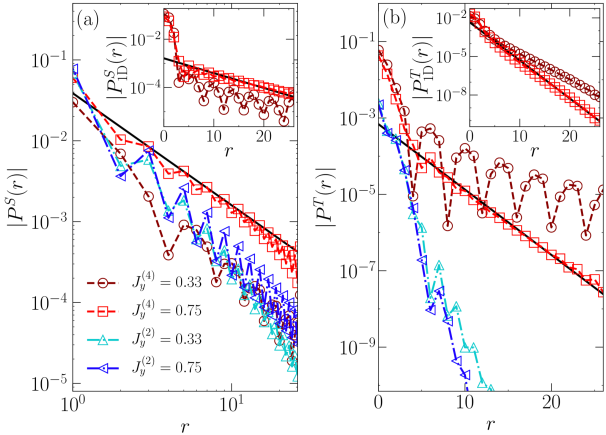

$$P(r) = \frac{1}{\sqrt{\mathcal{N}}} \sum_{|x_1 - x_2| = r} P_{x_1, x_2}$$

Simulation results II

LegNum	J_y	P^S	P^T	P^S_{1D}	P^T_{1D}
2	0.33	∼pow	exp	x	x
2	0.75	∼pow	exp	x	x
4	0.33	∼pow	∼pow	exp	EXP
4	0.75	POW	exp	EXP	exp

- For anisotropic exchange couplings, four-legs ladder with a Mott stripe in the inner two legs exhibit singlet-pair superfluidity with the fermions in the pair being on opposite legs about the Mott insulating stripe.
- The presence of the Mott stripe in the inner two legs of the four-legs ladder for the occurrence of singlet-pair superfluidity between legs with $\langle \hat{n}_i \rangle \approx 0.5$ is important.

Definitions

One-particle correlation

$$\rho_{x_1,x_2} = \langle \hat{c}^{\dagger}_{x_1,1,\downarrow} \hat{c}_{x_2,1,\downarrow} \rangle$$

spin-spin correlation

$$S^z_{x_1,x_2} = \langle \hat{S}^z_{x_1,1} \hat{S}^z_{x_2,1} \rangle$$

Simulation results I

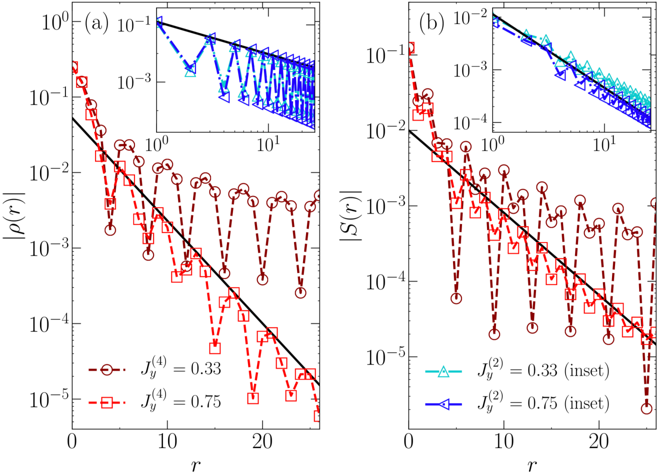

Simulation results II

- For four-legs ladder with anisotropic exchange, the single-particle and spin excitations are gapped in the singlet-pair superfluid phase.
- In the anisotropic case in two-legs ladder, there is a competition between one-particle, spin-spin, and inter-leg singlet-pair correlations, all of which are found to decay algebraically.

Section summary

Results

- for anisotropic exchange couplings, an inter-leg singlet-pair superfluid phase occurs.
- The singlet-pair superfluid phase is characterized by a negative binding energy, algebraically decaying inter-leg singlet-pair correlations and exponentially decaying inter-leg triplet-pair correlations, intra-leg singlet- and triplet-pair correlations, as well as intra-leg one-particle and spin-spin correlations.

About the Mott insulating stripe

- It has antiferromagnetic correlations that mediate the interaction between the fermions in outer two legs such that they form singlets.
- Because of the double-occupancy constraint, the Mott strip constrains the motion of the fermions in the outer legs to be one dimensional, which makes the singlet-pair phase robust against delocalization of the fermions across the legs.

Hamiltonian

t-t'-J model

$$
\begin{aligned}
H = & -t \sum_{\boldsymbol{l},\boldsymbol{\delta},\sigma} (c^\dagger_{\boldsymbol{l}+\boldsymbol{\delta},\sigma} c_{\boldsymbol{l},\sigma} + c^\dagger_{\boldsymbol{l}-\boldsymbol{\delta},\sigma} c_{\boldsymbol{l},\sigma}) \\
& -t' \sum_{\boldsymbol{l},\boldsymbol{\delta}',\sigma} (c^\dagger_{\boldsymbol{l}+\boldsymbol{\delta}',\sigma} c_{\boldsymbol{l},\sigma} + c^\dagger_{\boldsymbol{l}-\boldsymbol{\delta}',\sigma} c_{\boldsymbol{l},\sigma}) \\
& +J \sum_{\boldsymbol{l},\boldsymbol{\delta}} (\boldsymbol{S}_{\boldsymbol{l}+\boldsymbol{\delta}} \cdot \boldsymbol{S}_{\boldsymbol{l}} - \frac{1}{4} n_{\boldsymbol{l}+\boldsymbol{\delta}} n_{\boldsymbol{l}})
\end{aligned}
$$

$t > 0$ and $t' < 0$ for hole doping; $t < 0$ and $t' > 0$ for electron doping.

Parameters

System parameters

L_x	L_y	BC	$J/\|t\|$	t'/t	$x_{h(e)} = n_{h(e)}/96$
24	4	XOBC YPBC	0.4	-0.25	1/12 1/8 1/6

Simulation parameters

MaxStateNum	TruncErr
4000	3×10^{-4}

Observables

Dynamic charge structure factor

$$C_{\boldsymbol{l}}^{n+}(t) \propto -i\langle 0|[\tilde{n}_{\boldsymbol{l}}(t), \tilde{n}_{\mathbf{0}}(0)]|0\rangle$$

where $\tilde{n}_{\boldsymbol{l}} \equiv n_{\boldsymbol{l}} - \langle 0|n_{\boldsymbol{l}}|0\rangle$

$$C^{n+}(\boldsymbol{q}, \omega) \propto \int e^{i\omega t - \gamma|t|} e^{-\boldsymbol{q}\cdot\boldsymbol{l}} C_{\boldsymbol{l}}^{n+}(t)$$

$$N(\boldsymbol{q}, \omega) = -\frac{1}{\pi}\mathrm{Im}C^{n+}(\boldsymbol{q}, \omega)$$

Dynamical spin structure factor

$$S(\boldsymbol{q}, \omega) = -\frac{1}{\pi}\mathrm{Im}C^{S^z+}(\boldsymbol{q}, \omega)$$

Carrier distribution in the ground state I

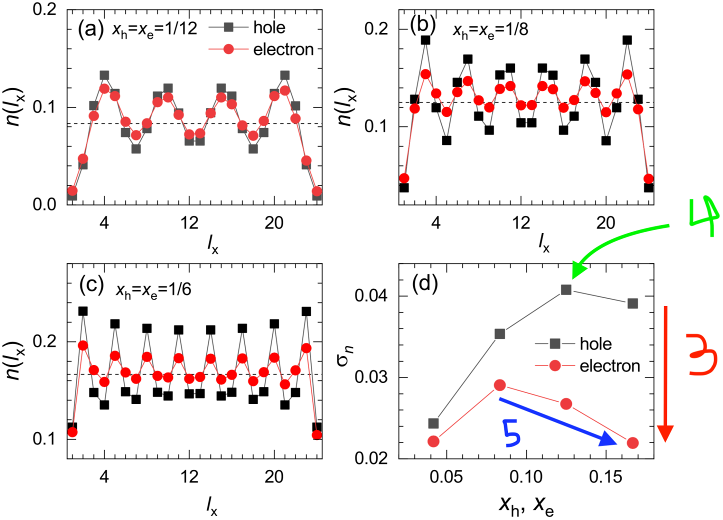

Carrier distribution in the ground state II

1. An oscillation of $n(l_x)$ in the middle of the ladder, depending on the charge density in both hole and electron dopings.
2. The oscillation period is given by $(2x_{h(e)})^{-1}$.
3. The amplitude of the oscillation is smaller in electron doping than in hole doping.
4. In hole doping, the strongest stripe order appears near the 1/8 doping, which is observed in hole doped cuprates.
5. In electron doping, stripe order is small and decreases above $x_e = 1/12$
6. Spin density is zero in all cases.

Dynamical charge structure factor

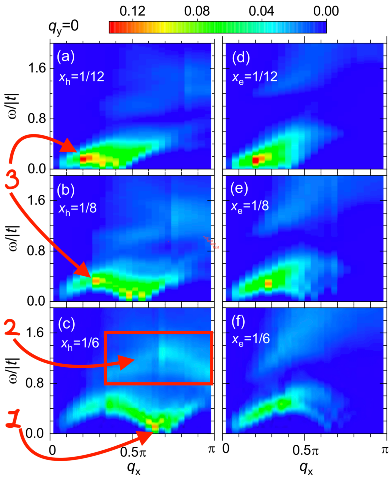

1. Strong low-energy excitations with broadening whose energy minimum is located around $q_x = 4x_h\pi$ emerge in the hole-doped case.
2. High-energy excitations above $\omega = 0.8|t|$ show broad dispersive features that are steeper than those in hole doping.
3. Strong low-energy excitations for small $\boldsymbol{q}$ at the low doping region in $N(\boldsymbol{q}, \omega)$.

Dynamical spin structure factor ($q_y = \pi$) I

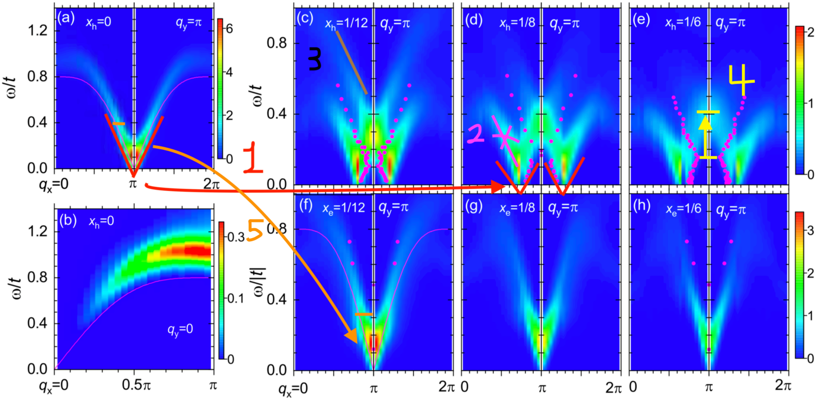

Dynamical spin structure factor ($q_y = \pi$) II

1. With hole doping the $\boldsymbol{q} = (\pi, \pi)$ excitation at half filling splits into two low-energy excitations along the $(0, \pi) - (\pi, \pi)$ direction.
2. Linear dispersive branches emerge from the q_x position toward both the $q_x = \pi$ (inward) and $q_x = 0$ (outward) directions. But in In inelastic neutron scattering (INS), the outward dispersion has not been observed. This inconsistency may arise from ladder geometry.
3. There is a linear dispersive structure with small intensity extending up to $\omega \sim t$.
4. Contrast with experimental peaks, the neck position of the hour-glass dispersion is higher in the calculated (π, π) spectrum.
5. In electron doping, the dispersive behavior near (π, π) is similar to that at half filling, but away from (π, π) the spectral distribution becomes broader.

Integrated weight of $S(\boldsymbol{q}, \omega)$ I

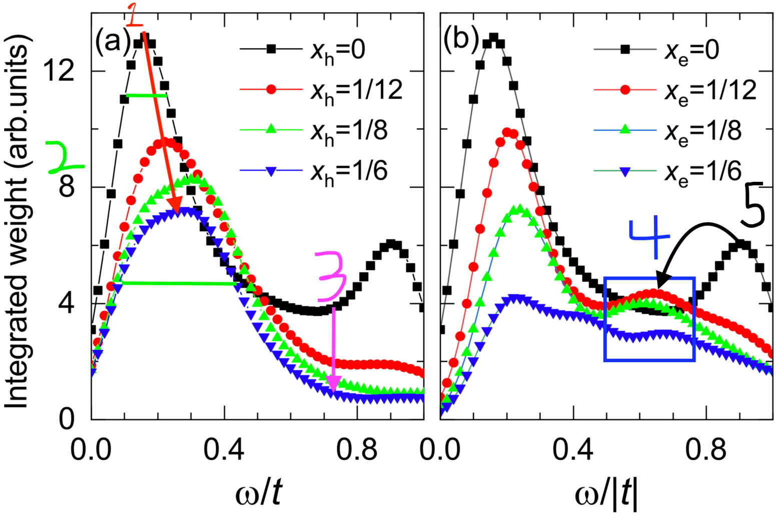

Integrated weight of $S(\boldsymbol{q},\omega)$ II

1. In hole doping, the lowest-energy peak reduces its weight with x_h.
2. The peak broadens with extending the weight higher energy.
3. The energy region higher than J looses the weight significantly.
4. The weight at the high-energy region in electron doping remains less x_e dependent.
5. In electron doping, a high-energy peak at $0.9|t|$ at half filling shifts to the lower-energy side around $0.7|t|$ with increasing x_e.

Dynamical spin structure factor ($q_y = 0$) I

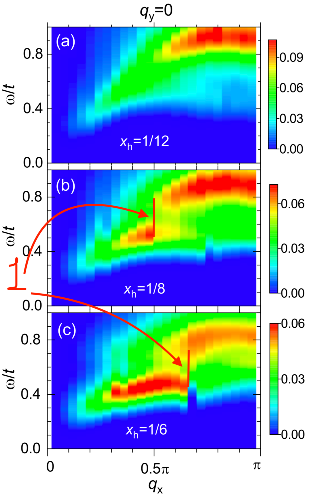

1. For $x_h = 1/8(1/6)$, discontinuous spectral intensity appears at $q_x \sim 4x_h\pi$ close to the stripe wave vector.
2. The anomaly near teh stripe wave vector in spin excitation has been reported in RIXS experiment, although clear discontinuous spectral intensity has not been identified.

Dynamical spin structure factor ($q_y = 0$) II

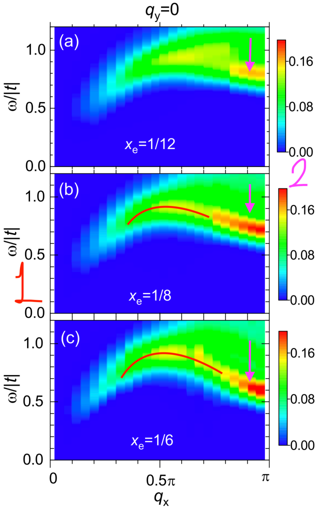

1. In electron doping, such a discontinuous behavior is invisible in $S(\boldsymbol{q}, \omega)$.
2. A downward shift of the peak position of spectral weight beyond $q_x \sim 0.5\pi$ for all three x_e case can be found in electron doping.
3. The signature of such a downward shift has not clearly been seen in the experimental data.

Section summary

- $N(\boldsymbol{q}, \omega)$ along the (0,0)-(π,0) direction clearly shows the low-energy excitations corresponding to the stripe order in hole doping, while the stripe order weaken in electron doping.
- In $S(\boldsymbol{q}, \omega)$, incommensurate spin excitations near the magnetic zone center $\boldsymbol{q} = (\pi, \pi)$ forming a hour-glass behavior in hole doping.
- In electron doping, clear spin-wave-like dispersions are seen.
- Along the (0,0)-(π,0) direction, the spin excitations are strongly influenced by the stripes in hole doping.
- The spin excitations show a downward shift in energy toward (π,0).

Summary

1. Exotic toy models may enhance novel behaviors, which can help us study the mechanism of strongly correlated systems.
2. Two dimensional t-(t')-J model is a mighty candidate for describing cuprate high-Tc superconductor.

Thank You!